01 May 2005

Wide-Band Lorentzian Media in the FDTD Algorithm

Marina Koledintseva
Missouri University of Science and Technology, marinak@mst.edu

James L. Drewniak
Missouri University of Science and Technology, drewniak@mst.edu

David Pommerenke
Missouri University of Science and Technology, davidjp@mst.edu

Giulio Antonini

et. al. For a complete list of authors, see https://scholarsmine.mst.edu/ele_comeng_facwork/1332

Recommended Citation

M. Koledintseva et al., "Wide-Band Lorentzian Media in the FDTD Algorithm," *IEEE Transactions on Electromagnetic Compatibility*, vol. 47, no. 2, pp. 392-399, Institute of Electrical and Electronics Engineers (IEEE), May 2005.
The definitive version is available at https://doi.org/10.1109/TEMC.2005.847406

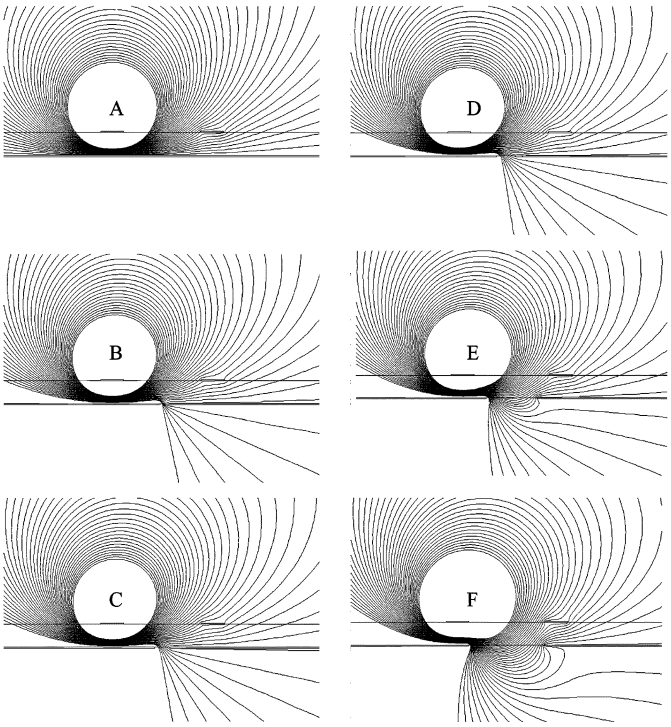

Fig. 11. Contour maps of the magnetic flux from test boards with varying width gaps in the return plane. (a) No gap. (b) $w_{gap} = 0.025$ cm. (c) $w_{gap} = 0.076$ cm. (d) $w_{gap} = 0.127$ cm. (e) $w_{gap} = 0.305$ cm. (f) $w_{gap} = 0.381$ cm.

VII. Conclusion

Gapping the return plane is an effective way to reduce or even eliminate common-impedance coupling between two parallel microstrip traces. However, a gap cut into the return plane has been shown to be ineffective at reducing capacitive and inductive coupling.

For capacitive coupling, experiments have shown that adding a gap in the return plane actually increases the mutual capacitance. However, the change is rather insignificant unless the width of the gap is quite large.

Two factors determine the effect of the gap on inductive coupling, the length of the gap and the width of the gap. Experiments show that if the gap is long enough to prevent current from flowing underneath the victim trace, then the mutual inductance may decrease slightly ($\sim$2 dB). When the gap is widened, there is a slight increase in inductive coupling. However overall, the gap has relatively little effect on inductive coupling.

To reduce crosstalk between circuits on a printed circuit board at frequencies below a few hundred kilohertz, where common-impedance coupling is likely to dominate, it may be advisable to gap the current return plane. However, gapping the return plane is not likely to reduce crosstalk at frequencies above a few hundred kilohertz where inductive and capacitive coupling dominate.

References

[1] C. R. Paul, *Introduction to Electromagnetic Compatibility*. New York: Wiley, 1992.

[2] C. Christopoulos, *Principles and Techniques of Electromagnetic Compatibility*. Boca Raton, FL: CRC, 1995, pp. 221–245.

[3] B. Archambeault, "Proper design of intentional splits in the ground reference plane of PC boards to minimize emissions on I/O wires and cables,," in *Proc. Int. Symp. Electromagnetic Compatibility*, Denver, CO, Aug. 1998, pp. 768–773.

[4] D. M. Hockanson, J. L. Drewniak, T. H. Hubing, T. P. Van Doren, F. Sha, C. W. Lam, and L. Rubin, "Quantifying EMI resulting from finite-impedance reference planes," *IEEE Trans. Electromagn. Compat.*, vol. 39, no. 3, pp. 225–232, Aug. 1997.

[5] C. L. Holloway and E. F. Kuester, "Net and partial inductance of a microstrip ground plane," *IEEE Trans. Electromagn. Compat.*, vol. 40, no. 1, pp. 33–46, Feb. 1998.

[6] W. Cui, H. Shi, X. Luo, J. L. Drewniak, T. P. Van Doren, and T. Anderson, "Lumped-element sections for modeling coupling between high-speed digital and I/O lines," in *Proc. Int. Symp. Electromagnetic Compatibility*, Austin, TX, Aug. 1997, pp. 260–265.

[7] Maxwell 2-D Extractor Ver. 4.0.04 and Ansoft HFSS Ver 6.0, Ansoft Corporation, Pittsburgh, PA, 1998.

Wide-Band Lorentzian Media in the FDTD Algorithm

Marina Y. Koledintseva, James L. Drewniak, David J. Pommerenke, Giulio Antonini, Antonio Orlandi, and Konstantin N. Rozanov

***Abstract*—This paper considers the case of a wide-band Lorentzian (WBL) algorithm in the finite-difference time-domain (FDTD) modeling of dispersive media. It is shown herein that the WBL model is a physically meaningful and practically useful case of the frequency behavior of materials along with the Debye and narrow-band Lorentzian (NBL). The recursive convolution algorithms for the finite-difference time-domain technique for NBL and WBL models differ. The Debye model, which is suitable for comparatively low-frequency dispersive materials, may not have sufficient number of parameters for describing the wide-band material, especially if this material exhibits pronounced absorption at higher frequencies. It is shown that the Debye model can be used, if the Q-factor of the linear circuit analog corresponding to the Lorentzian model of the material is less than approximately 0.8. If the quality factor is in the limits of about $0.8 < Q \leq 1$, then the WBL model is appropriate. For $Q > 1$, the NBL model must be applied. The NBL model is suitable for dielectrics exhibiting resonance effects in the microwave frequency range. The WBL model is typical for composites filled with conducting fibers.**

***Index Terms*—Debye model, dispersive media, finite-difference time-domain (FDTD) technique, Lorentzian model, recursive convolution.**

I. Introduction

The finite-difference time-domain (FDTD) method applied to the analysis of complex electromagnetic structures, including those containing dispersive composite dielectric, magnetic, and magnetodielectric media, has become widespread because of its robustness and comparative simplicity [1]–[3]. It is known that for linear dispersive media, the linear recursive convolution (LRC) approach is computationally effective, straightforward to implement and, therefore, attractive [1]–[4]. To implement the LRC or piecewise linear recursive convolution (PLRC) procedure, the frequency dependence of the material dielectric or magnetic susceptibility must be a rational function

Manuscript received February 9, 2004; revised August 28, 2004.

M. Y. Koledintseva, J. L. Drewniak, and D. J. Pommerenke are with the EMC Laboratory, University of Missouri, Rolla, MO 65409 USA (e-mail: marinak@umr.edu).

G. Antonini and A. Orlandi are with the Department of Electrical Engineering, University of L'Aquila, Poggio di Roio, 67040 AQ, Italy (e-mail: antonini@ing.univaq.it).

K. N. Rozanov is with the Microwave Laboratory of the Institute for the Theoretical and Applied Electromagnetics, Russian Academy of Sciences, 125412 Moscow, Russia (e-mail: k_rozanov@mail.ru).

Digital Object Identifier 10.1109/TEMC.2005.847406

to have a causal inverse Fourier (or Laplace) transform, which can be expressed as a sum of complex exponentials of time with constant coefficients. The simplest cases of such functions are Debye and Lorentzian frequency dependences [5], [6]. Luebbers *et al.* introduced both single- and multipole Debye and Lorentzian models into FDTD recursive convolution procedures [1], [4], [7]. Unlike the Debye case, where the convolution function of the susceptibility and field is real and straightforward to implement for a recursive procedure, in the Lorentzian model in the general case it is a complex function.

It is shown in this paper that depending on the ratio of a Lorentzian resonance line half-width δ (at the -3-dB level), and the resonance frequency ω_0, different recursive convolution equations and coefficients for field updating are needed. When $\delta/\omega_0 > 1$, it is defined herein as a wide-band Lorentzian (WBL) material, and for $\delta/\omega_0 < 1$, as a narrow-band Lorentzian (NBL) material, suitable for resonance effects and highly absorbing media modeling. The borderline case $\delta = \omega_0$ is not subjected to recursive convolution, and can be modeled as either WBL or NBL material.

The circuit-theory analogues for the simplest material models, Debye and Lorentzian, are well known [8]. Thus, a Debye model is an RC- or an RL-circuit, and a Lorentzian model is an RLC-circuit, as illustrated in Fig. 1. The quality factor of the RLC-circuit is $Q = \omega_0/\delta < 1$ for a WBL material, and $Q > 1$ for a NBL.

Though the linear circuit analogy for the dispersive media behavior was determined long ago [8], previous publications on FDTD modeling have not identified wide-band (WB) materials from the general group of Lorentzian media for recursive convolution algorithms [1]–[4]. Previous work reported on the FDTD modeling of Lorentzian media [1]–[4], [7] focused on the narrow-band (NB) case where the time-domain susceptibility kernel (or impulse response) of a medium was a damped oscillating function of time. However, the WBL model is a practically useful case of the material frequency behavior, and the FDTD NBL algorithm cannot be adapted for WB material modeling automatically just by changing the width of the resonance line as an input parameter. At the same time, the Debye model, which is suitable for comparatively low-frequency dispersive materials, does not have a sufficient number of parameters for the description of the WB material. The distinct behavior of these three dependencies is most readily seen from the circuit analogy and responses shown in Fig. 1.

The WBL behavior of permittivity is observed in fiber-filled composites at microwave frequencies [9]. Frequency characteristics of some magnetic materials can also be described by the WBL dispersion law [10], [11]. The frequency dependence in the WBL model for $Q \ll 1$ resembles that of a Debye model. The difference appears in the vicinity of the resonance frequency. With the Q-factor approaching unity, the difference between the two models becomes larger. In any case, a WBL model may be necessary for a detailed analysis, especially if the frequency range of interest is broad.

In Section II of this paper, the susceptibility kernels for the NBL and WBL models are represented in a form convenient for recursive convolution. Some examples of modeled and measured S-parameters for parallel-plate test boards with Debye, WBL, and NBL dielectrics are presented in Section III.

II. Updating Equations for Recursive Convolution

Most physical frequency dispersion laws for relative permittivity can be fitted by a sum of Lorentzian and Debye terms

$$\varepsilon_r(\omega) = \varepsilon_\infty + \sum_{k=1}^{M} \frac{A_k \omega_{0k}^2}{\omega_{0k}^2 - \omega^2 + j\,\omega 2\delta_k} + \sum_{i=1}^{N} \frac{B_i}{1 + \mathrm{j}\omega\tau_i} - \frac{\mathrm{j}\sigma_e}{\varepsilon_0 \omega} \quad (1)$$

where the second term on the right-hand side is responsible for the Lorentzian frequency dispersion, the third term introduces the Debye behavior, and the last term is responsible for the macroscopic ohmic loss in the material. In (1), ε_0 is the permittivity of vacuum; ε_∞ is the total high-frequency (or "optical") permittivity; $A_k\omega_{0k}^2 = (\varepsilon_{sk} - \varepsilon_\infty)\omega_{0k}^2$ and $B_i = \varepsilon_{si} - \varepsilon_\infty$ are, respectively, the real amplitudes for the Lorentzian or Debye resonance lines, where ε_{sk} is the static dielectric constant; ω_{0k} and $2\delta_k$ are the resonance frequency and the width of the kth Lorentzian peak, respectively; τ_i is the loss constant for the ith Debye component; and σ_e is the ohmic (dc) conductivity. The sum on the right-hand side of (1) is a rational function that can fit most dispersion laws obeying the Kramers–Kronig relations [5], with high accuracy.

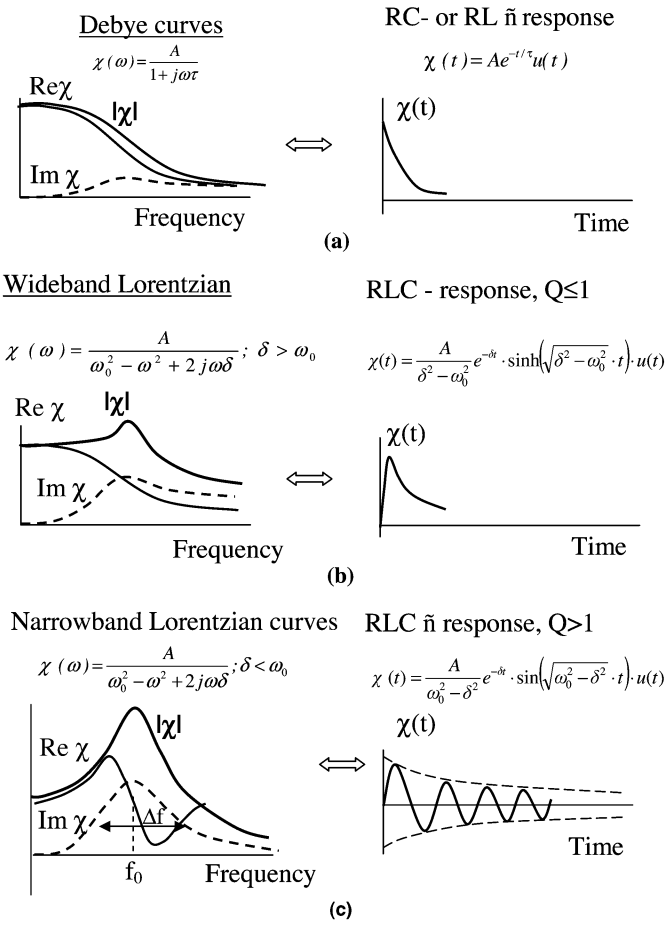

Fig. 1. Material models in frequency- and time-domains and circuit-theory analogues: (a) Debye model; (b) WBL model; (c) NBL model.

For the sake of simplicity, consider a single-component linear, isotropic, homogeneous dielectric material, with a frequency-dependent susceptibility that is described by a single-peak Lorentzian curve (second term in (1) with the index $k = 1$). Along the imaginary axis $s = j\,\omega$ of the complex plane $(\alpha, j\,\omega)$, its poles are

$$s_{1,2} = -\delta \pm \sqrt{\delta^2 - \omega_0^2}. \quad (2)$$

There may be three cases, depending on the complexity of the roots of (2): one real root; two different real roots; and two different complex roots. The degenerate case with $\omega_0 = \delta$ for a single pole $s = -\delta$ will not be considered here, because the susceptibility function in this case has a form $\chi(t) = At \cdot \exp(-\delta t) \cdot u(t)$, which cannot be treated by a recursive convolution procedure. Practically, the borderline case $\omega_0 = \delta$ frequency dependence of a material can be approximated by either a NBL or a WBL curve; however, it is reasonable to consider this case as a wideband, since it will yield the nonoscillating solution.

When $\omega_0 > \delta$, this is a *narrowband Lorentzian medium*, the roots of (2) are complex, and the dielectric susceptibility kernel $\chi_{\mathrm{NBL}}(t)$ is an oscillating function vanishing as $t \to \infty$

$$\chi_{\mathrm{NBL}}(t) = \frac{(\varepsilon_S - \varepsilon_\infty)\omega_0^2}{\Omega} \cdot \exp(-\delta \cdot t) \cdot \sin \Omega \mathrm{t} \cdot u(t) \tag{3}$$

where $\Omega = \sqrt{\omega_0^2 - \delta^2} \neq 0$, and $u(t)$ is a unit step-function.

The static susceptibility χ_0 can be represented as

$$\chi_0 = \int_0^{\Delta \mathrm{t}} \chi(t)dt = \frac{\varepsilon_s - \varepsilon_\infty}{\Omega} \cdot \begin{pmatrix} \Omega\,(1 - \exp(-\delta\Delta t)\cos \Omega\Delta \mathrm{t}) - \\ \delta \exp(-\delta\Delta t)\sin \Omega\Delta \mathrm{t} \end{pmatrix}. \tag{4}$$

For simplicity, consider the LRC procedure, though the PLRC is similar and straightforward [3]. When the medium is NBL, the convolution function $\vec{\Psi}$ [1], [2], [7] in the FDTD updating equations for the components of field along all three axes x, y, and z is complex. The updating equations for the E-field can be found in [2], [3] and represented here in a compact form as

$$\vec{E}^{n+1}(m) = A_\varepsilon \cdot \vec{E}^n(m) + B_\varepsilon \cdot \left(\nabla_d \times \vec{H}^{n+\frac{1}{2}} - \vec{J}^n(m)\right) + C_\varepsilon \vec{\Psi}(m) \tag{5}$$

where m denotes a node (i, j, k), and $\nabla_d \times$ is the discrete curl operator derived from applying central differencing on H-field in space [2]. The nth time step is $n = [t_n/\Delta t]$, where [ ] is the integer part. The vector $\vec{J}^n(m)$ describes an impressed electric current source. The coefficients A_ε, B_ε, and C_ε are [2]

$$A_\varepsilon = \frac{\varepsilon_0\varepsilon_\infty}{\varepsilon_0(\varepsilon_\infty + \chi_0) + \sigma_e\Delta \mathrm{t}}; \quad B_\varepsilon = \frac{\varepsilon_0 \cdot \Delta \mathrm{t}}{\varepsilon_0(\varepsilon_\infty + \chi_0) + \sigma_e\Delta \mathrm{t}};$$
$$C_\varepsilon = \frac{\varepsilon_0}{\varepsilon_0(\varepsilon_\infty + \chi_0) + \sigma_e\Delta \mathrm{t}}. \tag{6}$$

If the medium is considered as nonmagnetic or with nondispersive permeability, then the equation for the magnetic field updating is the same as in [2], and in the compact vector form is

$$\vec{H}^{n+\frac{1}{2}}(m) = A_\mu \vec{H}^{n-\frac{1}{2}}(m) + B_\mu \cdot \nabla_d \times \vec{E}^n \tag{7}$$

where $A_\mu = 1$ and $B_\mu = \Delta t/(\mu_0\mu)$.

The real and imaginary parts for the NBL case are coupled as

$$\mathrm{Re}\vec{\Psi}^{n+1} = \vec{E}^{n+1} \cdot \mathrm{Re}(\Delta\chi^0) + \exp(-\delta\Delta t) \cdot (\mathrm{Re}\vec{\Psi}^{\mathrm{n}} \cdot \cos \Omega\Delta \mathrm{t} - \mathrm{Im}\vec{\Psi}^{\mathrm{n}} \cdot \sin \Omega\Delta \mathrm{t}) \tag{8}$$

and

$$\mathrm{Im}\vec{\Psi}^{n} = \vec{E}^{n} \cdot \mathrm{Im}(\Delta\chi^0) + \exp(-\delta\Delta t) \cdot (\mathrm{Im}\vec{\Psi}^{\mathrm{n}-1} \cdot \cos \Omega\Delta \mathrm{t} + \mathrm{Re}\vec{\Psi}^{\mathrm{n}-1} \cdot \sin \Omega\Delta \mathrm{t}) \tag{9}$$

where the real and imaginary parts of the susceptibility increment are

$$\mathrm{Re}(\Delta\chi^0) = \frac{\varepsilon_s - \varepsilon_\infty}{\Omega} \cdot \begin{pmatrix} \Omega(1 - 2\exp(-\delta\Delta t)\cos \Omega\Delta \mathrm{t} + \\ \exp(-2\delta\Delta t)\cos 2\Omega\Delta \mathrm{t}) - \\ \delta(2\exp(-\delta\Delta t)\sin \Omega\Delta \mathrm{t} - \\ \exp(-2\delta\Delta t)\sin \Omega\Delta \mathrm{t}) \end{pmatrix} \tag{10}$$

and

$$\mathrm{Im}(\Delta\chi^0) = \frac{\varepsilon_s - \varepsilon_\infty}{\Omega} \cdot \begin{pmatrix} -\delta(1 - 2\exp(-\delta\Delta t)\cos \Omega\Delta \mathrm{t} + \\ \exp(-2\delta\Delta t)\cos 2\Omega\Delta \mathrm{t}) - \\ \Omega(2\exp(-\delta\Delta t)\sin \Omega\Delta \mathrm{t} - \\ \exp(-2\delta\Delta t)\sin 2\Omega\Delta \mathrm{t}) \end{pmatrix}. \tag{11}$$

The case for $\omega_0 < \delta$ corresponds to a WBL medium. It should be noted that the resonance frequency ω_0 in the WBL case, in contrast to the NBL case, might differ greatly from the location of the absorption peak in the material. The poles of the Lorentzian function in (1) are real

$$s_{1,2} = -\delta \pm \nu \tag{12}$$

where $\nu = \sqrt{\delta^2 - \omega_0^2} \neq 0$.

The susceptibility kernel $\chi_{\mathrm{WBL}}(t)$, found according to the Heaviside formula [12] used for calculating inverse Laplace transforms of fractional rational functions, is a nonoscillating damped function

$$\chi_{\mathrm{WBL}}(t) = (\varepsilon_s - \varepsilon_\infty)\omega_0^2 \left(\frac{\exp(s_1 t)}{s_1 + \delta} + \frac{\exp(s_2 t)}{s_2 + \delta}\right) = (\varepsilon_s - \varepsilon_\infty)\omega_0^2 e^{-\delta t}\frac{\sinh(\nu \mathrm{t})}{\nu}. \tag{13}$$

The static susceptibility is

$$\chi_0 = \frac{(\varepsilon_s - \varepsilon_\infty)\omega_0^2}{2\nu}\left(-\frac{\exp(-\xi_1\Delta \mathrm{t}) - 1}{\xi_1} + \frac{\exp(-\xi_2\Delta \mathrm{t}) - 1}{\xi_2}\right) \tag{14}$$

where $\xi_{1,2} = \delta \mp \nu$.

Then the convolution function is a difference of two separate recursively calculated real terms

$$\vec{\Psi}^n = \vec{\Psi}_1^n - \vec{\Psi}_2^n \tag{15}$$

where the partial convolution functions are updated similar to that of a Debye medium [1],

$$\vec{\Psi}_{1,2}^n = \sum_{p=0}^{n-1} \vec{E}^{n-p} \cdot \Delta\chi_{1,2}^p = \vec{E}^n \Delta\chi_{1,2}^0 + \exp(-\xi_{1,2}\Delta \mathrm{t})\vec{\Psi}_{1,2}^{n-1} \tag{16}$$

with the susceptibility increments

$$\Delta\chi_{1,2}^0 = \frac{(\varepsilon_s - \varepsilon_\infty)\omega_0^2}{2\nu} \cdot \frac{(\exp(-\xi_{1,2}\Delta \mathrm{t}) - 1)^2}{\xi_{1,2}}. \tag{17}$$

Since the recursive convolution procedure in the WBL model deals with real functions, it cannot be represented as the limiting case of the NBL model. It should be noted that the WBL curve is not equivalent to the superposition of two independent Debye terms. Though formally the WBL dependence in the frequency domain can be represented as the difference of two rational functions with first-order poles (Debye-like terms) as

$$\chi_{\mathrm{WBL}}(\omega) = \frac{\tilde{A}\omega_0^2}{\omega_0^2 - \omega^2 + 2j\omega\delta} = \frac{A_1}{1 + j\omega\tau_1} - \frac{A_2}{1 + j\omega\tau_2} \tag{18}$$

where $\omega_0^2 = 1/\tau_1\tau_2$; $2\delta = (1/\tau_1) + (1/\tau_2)$, and the amplitudes A_1 and A_2 are not arbitrary and not independent of each other. They are related by $A_1 = \tilde{A}\omega_0^2\tau_1^2\tau_2/(\tau_1 - \tau_2)$ and $A_2 = \tilde{A}\omega_0^2\tau_1\tau_2^2/(\tau_1 - \tau_2)$.

Actually, independent amplitudes in (18) can lead to results that lack a physical interpretation. In addition, (18) implies that one of the Debye-type susceptibilities introduced this way would have a negative static value. The difference of two Debye terms has no physical interpretation and is not used for characterization of materials. By contrast, the WBL curve describes a medium, which is physically meaningful. For example, this is a dielectric medium with inclusions having low conductivity and such a size and concentration that it is impossible to neglect their capacitance and inductance, and the dissipation is substantial. High loss in the material widens the resonance curve, damps the potential resonance amplitude, and shifts the frequency of maximum loss to lower frequencies. In addition, more complex material characteristics can be comprised as a superposition of WBL responses in a physically meaningful way.

The WBL case requires twice the memory for the computations as compared to the single Debye case. However, because of a greater number of parameters employed, the WBL model can better approximate the frequency behavior of some materials, and describes the response of the material analogous to an over-damped RLC-circuit with a low Q-factor. From the computational point of view, WBL, in contrast with the NBL model, does not deal with complex arithmetic, and this simplifies programming.

III. Numerical and Experimental Results

In this section, numerical data using FDTD algorithms for the Debye and both NBL and WBL dielectrics are presented, as well as a comparison with the corresponding experimental results.

A. Double-Sided Substrate With WBL and Debye Dielectric

Computations using a Debye and a WBL model were run for the copper-clad substrate, or double-sided printed circuit board containing an FR-4 (fiberglass—epoxy) dielectric layer, as shown in Fig. 2, in the frequency range from 100 MHz to 5 GHz. The board size was 150 mm $\times$ 200 mm, and the dielectric layer was 1.65 mm (65 mil) thick. Port 1 (30 mm, 125 mm) was located close to the board corner to excite as many modes of the parallel-plane waveguide as possible. Port 2 was selected arbitrarily and had coordinates (130 mm, 70 mm). Both test ports in the experimental board were built using $0.085''$ semi-rigid coaxial cables having outer shields soldered to the ground plane with a 360-degree connection. The center conductors extended through the thickness of the board, and were soldered to the opposite plane. SMA connectors were mounted on the other ends of the semi-rigid cables for the connection of test instruments.

The computational domain used in the FDTD simulation was discretized by a uniform mesh with the steps $\Delta x = \Delta z = 1$ mm, and $\Delta y = 0.165, 0.33,$ and 0.55 mm. Three, five, or ten FDTD cells were used across the board thickness; however, the number of the cells had no effect on the results for the given parallel-plate type excitation. A sinusoidally modulated 50-Ω Gaussian voltage source applied vertically above the ground plane was used in the simulations. The power and ground planes were modeled as perfect electric conductors (PECs) of zero thickness. Due to the relatively large thickness of the test board, the dielectric loss dominates, and the skin effect loss can be neglected. Eight perfectly matched layers (PML) were placed at each boundary plane of the computational domain, and seven free space layers were placed between the PML and the test board. The FDTD codes used double-precision numbers. Experimental data was obtained using a 37 275A Wiltron network analyzer, the frequency range of operation of which was 40 MHz–20 GHz. Fig. 3 demonstrates the necessity of taking into account the dispersive nature of dielectrics. The S-parameters of the board shown in Fig. 2 were measured and extracted

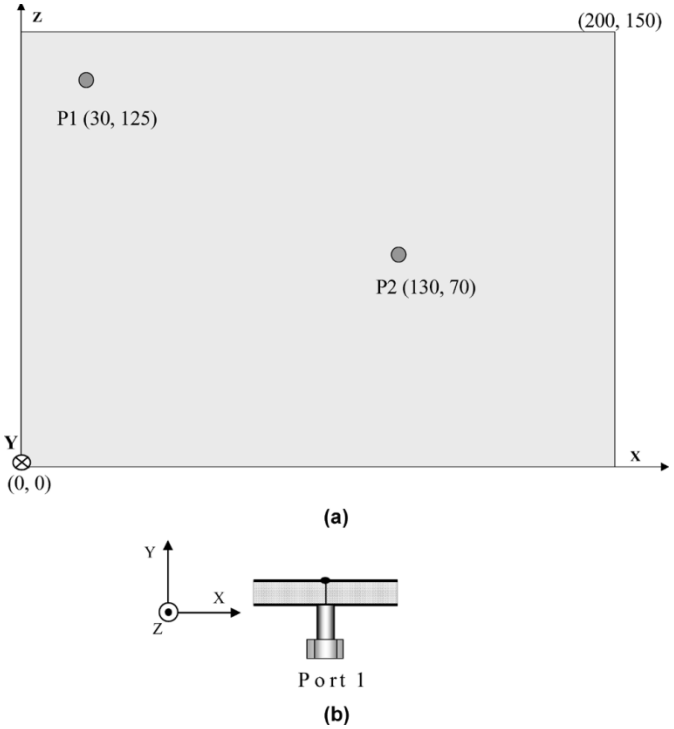

Fig. 2. Schematic of the test double-sided copper-clad substrate with dispersive dielectric in between: (a) top view and (b) profile at Port 1. All dimensions are in millimeters.

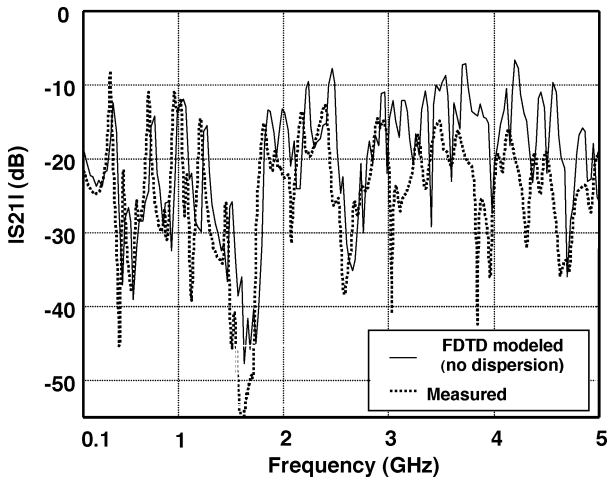

Fig. 3. Measured and FDTD modeled scattering matrix parameter $|S_{21}|$ for the test substrate without taking into account a dispersive nature of a dielectric, $\varepsilon_r = \text{const} = 4.3$ and $\sigma_e = 4 \cdot 10^{-3}$ S/m.

for the FDTD modeling of the FR-4 fiberglass epoxy. According to the low-frequency manufacturer's data, at 500 MHz the dielectric constant is $\varepsilon_r = 4.3$, and the loss tangent is $\tan\delta = 0.022$, corresponding to an effective conductivity $\sigma_e = 4 \cdot 10^{-3}$ S/m [13]. These low-frequency data were used for the modeling in the entire frequency range of interest (40 MHz–5 GHz), and the results of the computations failed to correspond with the measured results.

In most cases, parameters of Lorentzian or Debye curves are unknown, but reference or experimental data are often available at given frequencies. Frequently, measurements are conducted using NB cavity techniques [8], [14]. Parameters of a Debye or a Lorentzian dispersive dielectric can be obtained using measured, reference, or manufacturer's data at a few frequency points, as described in [15]–[17]. The Debye

curve for a dielectric with low-frequency conductivity loss is reconstructed from the data ε' and ε'' at two frequency points $\omega_{1,2}$ by solving the system of equations with four unknown variables ($\varepsilon_s\ \varepsilon_\infty, \tau_r, \sigma_e$). It is free from convergence problems, because it is based on an analytical solution of a corresponding system of nonlinear equations. Physical restrictions following from the fundamental Kramers–Kronig relations are applied [5]. For Lorentzian dielectrics, when the conductivity σ_e is not taken into account, four equations are needed to find four unknown parameters ε_s, ε_∞, δ, and ω_0 [18]. These may be measurements of both real and imaginary parts of susceptibility at two frequency points. Restrictions when solving such a system are that all the variables are real and positive, and $\varepsilon_s > \varepsilon_\infty$. However, if the conductivity term contributes significantly, then five equations are needed for extracting five unknowns (ε_s, ε_∞, δ, ω_0, and σ_e), which are required to be real and positive. As is stated in [15], if the number of experimental data available is larger than the number of unknown parameters, the accuracy of the dispersion curve reconstruction can be improved proportionally to the number of sample points. The system of equations is solved for multiple possible combinations of the experimental data (points), choosing the number of points equal to the number of the unknowns. Then, a reasonable combination of these results, e.g., weighted averaging, allows minimization of the uncertainty of the reconstructed parameter.

If the dispersion law of a material is characterized by a single Lorentzian term without an ohmic conductivity, the least mean square technique for the reconstruction of the parameters of dispersion curve is also available [17]. In this case, only dielectric loss is exploited which requires twice as much experimental data. To find the parameters of the Lorentzian curve, the experimental data are fit to the quadratic function. The fit uses the least mean square method that searches for the coefficients of the quadratic dependence by solving of a system of linear equation presented in [17]. This method of reconstruction is less cumbersome and more straightforward, and it was first developed to process the permittivity data obtained from the measured transmission coefficient of a resonance cavity [16].

Another method for the extracting parameters of the Debye and Lorentzian curves, as well as of their superposition, is based on the application of the genetic algorithms, as described in [19], [20].

Extracted Debye and WBL curves for real and imaginary parts of the permittivity of the FR-4 material are shown in Fig. 4(a)–(b). The extracted parameters for the WBL dielectric were $\varepsilon_s = 4.301$, $\varepsilon_\infty = 4.096$, $\sigma_e = 2.295 \cdot 10^{-3}$ S/m, $f_0 = 39.5$ GHz, and $\Delta f = 200$ GHz. Herein, $\Delta f = \delta/\pi$ is half of the resonance linewidth, and $f_0 = \omega_0/(2\pi)$ is the resonance frequency. A Debye material with a frequency dependence of permittivity close to the above WBL characteristics had the parameters of $\varepsilon_s = 4.301$, $\varepsilon_\infty = 4.096$, $\sigma_e = 2.295 \cdot 10^{-3}$ S/m, and $\tau_r = 2.320 \cdot 10^{-11}$ s. The experimental and the FDTD modeled scattering-matrix parameter $|S_{21}|$ of the described test board with FR4 modeled as the Debye and WBL dielectrics are shown in Fig. 5. For both the Debye and the WBL models, the FDTD-simulated and experimental data agree within 1–3 dB in amplitude (except for some nulls at higher frequencies), and the shift of resonance peaks is less than 5% in most of the frequency range. The similarity of the FDTD results with the Debye and WBL model is because the FR-4 is a low-loss dielectric used at comparatively low frequencies, where the material resonance effects are not very pronounced. In this example, the ratio $\delta/\omega_0 = 2.53$, or the quality factor is about $Q = 0.4$, which is considerably less than 1. However, at higher frequencies the WBL algorithm may be preferable even for FR-4, because of a greater number of parameters involved and more flexibility when approximating the parameters of the dielectric substrate.

An example of a material, for which the Debye model is insufficient, is shown in Fig. 6. This is a composite dielectric with a polymer matrix of $\varepsilon_r \approx 2.15$ filled with an aluminum powder.

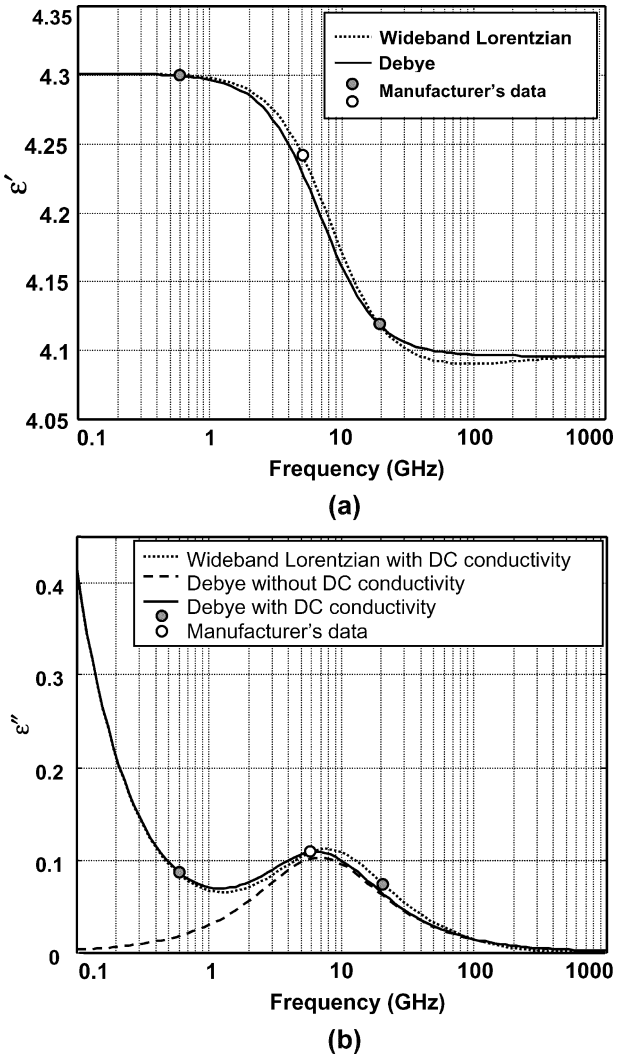

Fig. 4. Debye and Lorentzian dielectric models of a test substrate containing FR-4: (a) real part, and (b) imaginary part of permittivity. Parameters of the dielectrics for the Debye model are $\boldsymbol{\varepsilon_s = 4.301}$, $\boldsymbol{\varepsilon_\infty = 4.096}$, $\boldsymbol{\sigma_e = 2.294 \cdot 10^{-3}}$ S/m, and $\boldsymbol{\tau_r = 2.294 \cdot 10^{-11}}$ s. For the Lorentzian model, the parameters are $\boldsymbol{\varepsilon_s = 4.301}$, $\boldsymbol{\varepsilon_\infty = 4.096}$, $\boldsymbol{\sigma_e = 2.294 \cdot 10^{-3}}$ S/m, $\boldsymbol{\Delta f = 200}$ GHz, and $\boldsymbol{f_0 = 39.5}$ GHz.

The concentration of aluminum powder is 10%, and the diameter of the particles is 10–15 μm. The dielectric loss in the matrix is negligible. The composite material is produced by a spray painting layer-over-layer technology to build up thickness that can be on the order of submillimeter to millimeters. In the FDTD modeling, any effects of possible anisotropy are not taken into account.

A 0.8 mm thick sheet of this material was placed between two copper plates with dimensions of 100 mm × 75 mm. Ports 1 and 2 for the S-parameter measurement and the FDTD modeling had the coordinates in millimeters of (15, 63) and (65, 35), respectively. The composite is modeled as a WBL dielectric with the parameters $\varepsilon_s = 2.5$, $\varepsilon_\infty = 2.15$, Δf = 190 GHz, $f_0 = 85$ GHz, and $\sigma_e = 10^{-4}$ S/m. In this case, the ratio $\delta/\omega_0 = 1.12$, or $Q = 0.9$, which is near 1. The mesh for the FDTD modeling was chosen as 0.5 mm × 0.16 mm × 0.5 mm. The frequency range where measurements and modeling were made was from 40 MHz to 14 GHz. As seen in Fig. 6, the modeled curve with the WBL dielectric fits the experimental results well up to 6 GHz (within 3 dB of the amplitude, and the frequency shift of resonance peaks is less than 10%). At higher frequencies the discrepancy increases, but the model remains satisfactory (within 5 dB of the amplitude and less than 15% shift of resonance peaks). The Debye model with the parameters $\varepsilon_s = 2.5$, $\varepsilon_\infty = 2.15$,

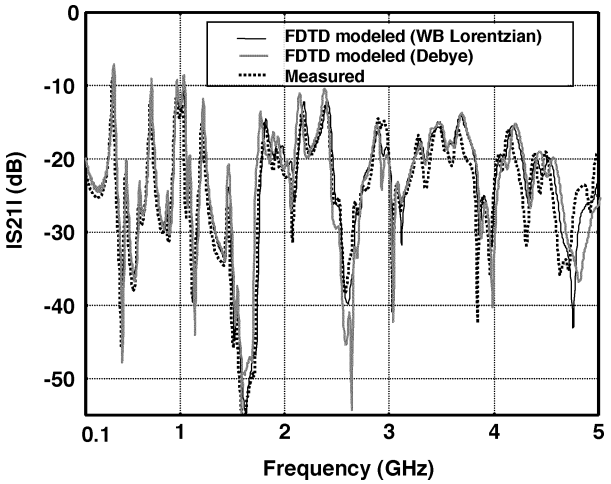

Fig. 5. Measured and FDTD modeled $|S_{21}|$ for the test substrate as a WBL dielectric with the parameters $\varepsilon_S = 4.301$, $\varepsilon_\infty = 4.096$, $\sigma_e = 2.294 \cdot 10^{-3}$ S/m, $f_0 = 39.5$ GHz, and $\Delta f = 200$ GHz, and as a Debye dielectric with the parameters $\varepsilon_S = 4.301$, $\varepsilon_\infty = 4.096$, $\sigma_e = 2.294 \cdot 10^{-3}$ S/m, and $\tau_r = 2.321 \cdot 10^{-11}$ s.

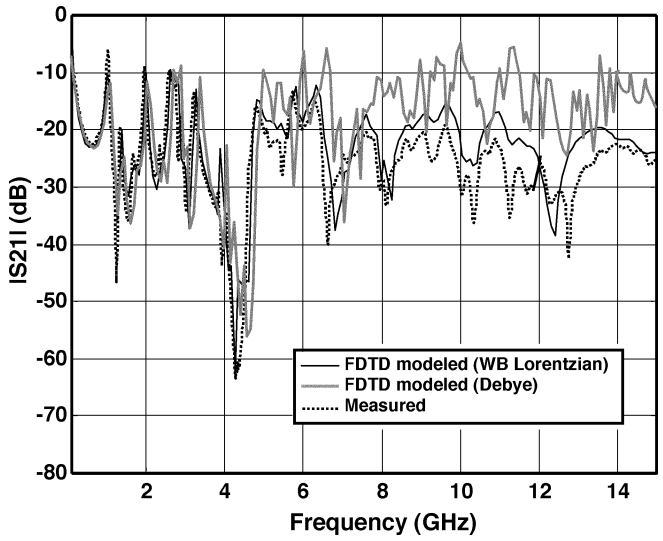

Fig. 6. Measured and FDTD modeled $|S_{21}|$ frequency dependence for a composite material as the WBL dielectric with the parameters $\varepsilon_s = 2.5$, $\varepsilon_\infty = 2.15$, $\Delta f = 190$ GHz, $f_0 = 85$ GHz, and as the Debye dielectric with the parameters $\varepsilon_s = 2.5$, $\varepsilon_\infty = 2.15$, $\tau_r = 2.5 \cdot 10^{-12}$ s. Conductivity in both cases was taken as $\sigma_e = 10^{-4}$ S/m.

$\tau_r = 2.5 \cdot 10^{-12}$ s, and $\sigma_e = 10^{-4}$ S/m that approximates the behavior of the same composite material, does not fit the experimental $|S_{21}|$ curve at higher frequencies. The amplitude discrepancy is approximately 20 dB, and the shift of resonance peaks is up to 50% in the frequency range of 6–15 GHz. This can be explained by an insufficient loss in the Debye model at higher frequencies. Therefore, the Debye model in this case is not suitable.

B. Comparison of Wide-Band and Narrow-Band Lorentzian Dielectric Behavior

Material resonance effects in FR-4 may take place only at frequencies of several tens of gigahertz, where FR-4 is presently not used and not characterized by manufacturers. Hence, fitting a NBL model for FR-4 is not presently achievable. However, the NBL model can be useful for full-wave analysis of structures containing high-loss composite media, for example, polymer composites with conducting fibers that find application as antistatic materials, electromagnetic shields, radar absorbers, etc. Such materials have pronounced dispersion in the microwave frequency band, and their effective permittivity behaves according to a single-pole or a multipole NBL law depending on the contents of the composite. The same material as shown in Fig. 7(a)–(b) of Lagarkov *et al.* [9], was used in the present study for NBL FDTD modeling. This is a two-phase composite, filled with aluminum-coated glass fibers (the fiber length is 8 mm; a volume concentration of 0.02%), and 10% of aluminum powder. The aluminum powder contains particles with sizes in the range of 10–15 μm. The aluminum-coated glass fibers have an overall thickness of approximately 25 μm, where the aluminum coating is approximately one-third of the glass fiber cross-section. The resistivity of the coating is assumed to be equal to that of bulk aluminum, 2.65 $\mu\Omega \cdot$ cm. The fibers are embedded in a polymer matrix of Teflon type having a dielectric constant $\varepsilon_r = 1.8$. The dielectric loss in the matrix is negligible. The technology of the material manufacturing was the same as of a WBL material described in Section III-A.

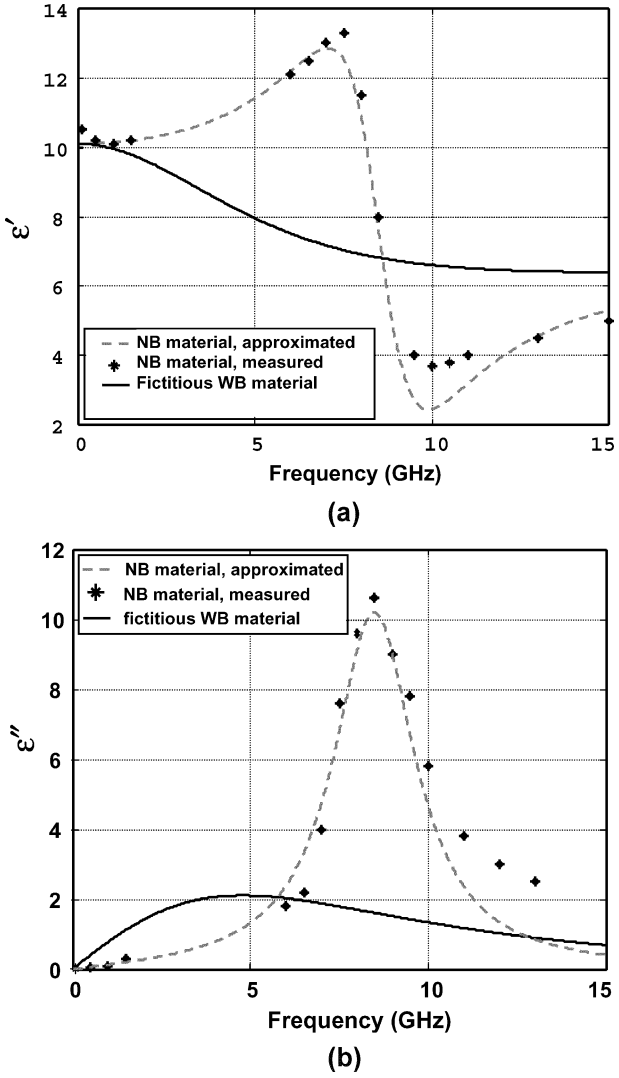

Fig. 7. Frequency dependence of (a) the real part of the permittivity, and (b) the imaginary part of permittivity for the Lorentzian dielectrics. Parameters for the WB dielectric material are $\varepsilon_S = 10.1$, $\varepsilon_\infty = 6.8$, $f_0 = 8.6$ GHz, $\Delta f = 17.8$ GHz, and for the NB dielectric material are $\varepsilon_S = 10.1$, $\varepsilon_\infty = 6.8$, $f_0 = 8.6$ GHz, $\Delta f = 2.8$ GHz. Conductivity is $\sigma_e = 0$ in both cases.

The experimental frequency characteristics of this NBL material are shown in Fig. 7(a)–(b) of the present paper. The fitted curve used in the FDTD models was determined by the least mean square method [16], [17]. The characteristics of a fictitious WBL material are also shown in Fig. 7(a)–(b) for comparison between the NB and WB behavior with

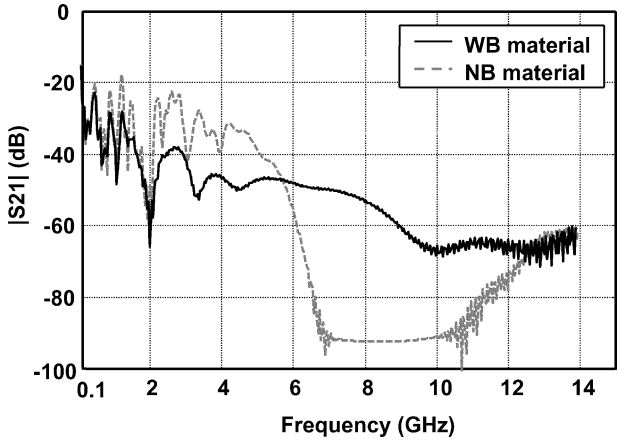

Fig. 8. Modeled frequency dependence of $|S_{21}|$ for the WB and the NBL dielectrics. Parameters of the WB and NB dielectrics are as in caption to Fig. 7.

FDTD modeling. The WB material has the same parameters as the NB, except for the width of the resonance line. For the WB material the ratio $\delta/\omega_0 = 1.03$, so that $Q = 0.96$, which is close to 1, and for the NB material the ratio $\delta/\omega_0 = 0.16$, and $Q = 6.1$. These materials—NB with parameters as in [9], and fictitious WB—were located between two metal perfect electric conducting planes for comparison in FDTD modeling. The geometry was similar to that in Fig. 2, but the size of the simulated board was 100 mm × 75 mm, and ports 1 and 2 had coordinates in millimeters of (15, 63) and (65, 35), respectively. This simple geometry of the structure is used only for FDTD modeling purposes.

The frequency dependences of $|S_{21}|$ for the NB and WB materials over the band of 100 MHz–15 GHz are represented in Fig. 8. The FDTD model of a test board with a NB Lorentzian material demonstrates a significantly greater number of resonances than the WB, as expected given the nature of the materials illustrated in Fig. 1. Multiple resonances due to the geometry of the two-sided copper-clad substrate are present only at lower frequencies where they are not damped significantly by the loss in the materials. At higher frequencies the NB material exhibits greater loss than the WB material, as follows from the difference in amplitude of ε_r'' for NB and WB materials shown in Fig. 7(b). The frequency characteristic of the NB material behaves as that of a band-reject filter, and the filtering effect of the WB material is less pronounced. Because of the material resonance effects, the NB algorithm requires at least 60 000 time steps, while the WB requires approximately 30 000. This is because of the longer high-Q-resonance "ringing" with the NBL model.

IV. Conclusion

The WBL model is a physically meaningful and a practically useful case for dielectric material frequency behavior. The FDTD NBL algorithm cannot be automatically used for WB material modeling just by changing the width of the resonance line as an input parameter. The Debye model, which is suitable for comparatively low-frequency dispersive materials, may not have enough parameters for describing the WB material, especially if this material exhibits absorption at higher frequencies.

Expressions for the recursive convolution procedure in the WBL case were derived, and they formally coincide with the recursive convolution of a subtraction of two Debye-like terms; however, these two terms are coupled. The parameters of the Lorentzian models are extracted from measurements for approximating the frequency-domain susceptibility functions in a form convenient for the recursive convolution procedure in the FDTD.

The FDTD computational results are presented for both WB and NBL models. It is shown that the FDTD simulations of a dielectric FR-4 (used in copper-clad substrates for printed circuit boards) in the frequency range below 5 GHz agree for the Debye and the WBL models and the experimental curves. This is due to the low Q-factor of the FR-4. The NBL model is suitable for fiber-filled composite dielectrics exhibiting resonance effects in the microwave frequency range. As compared to the Debye dielectric model, both Lorentzian models require more memory, but take into account resonance effects in the materials. The material frequency characteristic can be modeled as the Debye dependence, if the Q-factor of the corresponding Lorentzian model is less than approximately 0.8. If the quality factor is in the limits of about $0.8 < Q \leq 1$, then the WBL model is appropriate. For $Q > 1$, the NBL model must be applied.

From the computational point of view, in contrast with the NBL model, the WBL model does not deal with complex arithmetic, and that may be important for simplifying programming.

The WB and NBL models, together with the Debye model, are the full set of canonical media satisfying the causality principle. Implemented in the FDTD technique, they can be useful for the description of a wide variety of dielectric, magnetic, and magnetodielectric linear isotropic materials at higher frequencies in the microwave, millimeter wave, IR, and optical bands.

References

[1] K. S. Kunz and R. J. Luebbers, *The Finite Difference Time Domain Method for Electromagnetics*. Boca Raton, FL: CRC, 1993.
[2] A. Taflove, *Computational Electrodynamics: The Finite-Difference Time-Domain Method*. Norwood, MA: Artech House, 1995.
[3] A. Taflove and S. Hagness, *Computational Electrodynamics: The Finite-Difference Time-Domain Method*, 2nd ed. Norwood, MA: Artech House, 2000.
[4] R. J. Luebbers, F. P. Hunsberger, K. S. Kunz, R. B. Standler, and M. Schneider, "A frequency-dependent finite-difference time-domain formulation for dispersive materials," *IEEE Trans. Electromagn. Compat.*, vol. 32, no. 3, pp. 222–227, Aug. 1990.
[5] L. D. Landau, E. M. Lifshitz, and L. P. Pitaevskii, *Electrodynamics of Continuous Media*, 2nd ed. Oxford, NY: Pergamon, 1984.
[6] D. D. Pollock, *Physical Properties of Materials for Engineers*, 2nd ed. Boca Raton, FL: CRC, 1993.
[7] R. J. Luebbers and F. Hunsberger, "FDTD for Nth order dispersive media," *IEEE Trans. Antennas Propagat.*, vol. 40, no. 11, pp. 1297–1301, Nov. 1992.
[8] A. R. Von Hippel, *Dielectrics and Waves*. New York: Wiley, 1954.
[9] A. N. Lagarkov, S. M. Matytsin, K. N. Rozanov, and A. K. Sarychev, "Dielectric properties of fiber-filled composites," *J. Appl. Phys*, vol. 84, no. 7, pp. 3806–3814, Oct. 1998.
[10] A. V. Osipov, K. N. Rozanov, N. A. Simonov, and S. N. Starostenko, "Reconstruction of intrinsic parameters of a composite from the measured frequency dependence of permeability," *J. Phys. Condens. Matter*, vol. 14, no. 41, pp. 9507–9523, 2002.
[11] A. N. Lagarkov, K. N. Rozanov, N. A. Simonov, and S. N. Starostenko *et al.*, "Microwave permeability of magnetic films," in *Advanced Magnetic Materials*, Y. Liu *et al.*, Eds. Beijing, China: Tsinghua Univ. Press, 2004, vol. 3.
[12] G. A. Korn and T. A. Korn, *Mathematical Handbook for Scientists and Engineers; Definitions, Theorems, and Formulas for Reference and Review*. New York: McGraw-Hill, 1968.
[13] X. Ye, M. Y. Koledintseva, M. Li, and J. L. Drewniak, "FDTD modeling and design of a DC power-bus with dispersive media and surface mount technology components," *IEEE Trans. Electromagn. Compat.*, vol. 43, no. 4, pp. 579–587, Nov. 2001.
[14] J. Baker-Jarvis, E. J. Vanzura, and W. A. Kissick, "Improved technique for determining complex permittivity with the transmission/reflection method," *IEEE Trans. Microw. Theory Tech.*, vol. 38, no. 8, pp. 1096–1103, Aug. 1990.
[15] M. Y. Koledintseva, K. N. Rozanov, A. Orlandi, and J. L. Drewniak, "Extraction of the Lorentzian and Debye parameters of dielectric and magnetic dispersive materials for FDTD modeling," *J. Elect. Eng.*, vol. 53, no. 9/S, pp. 97–100, 2002.

[16] S. M. Matytsin, K. N. Rozanov, and N. A. Simonov, "Permittivity measurement using slotted coaxial resonator," in *Proc. IEEE 1996 Instrumentation and Measurement Technology Conf.*, Brussels, Belgium, Jun. 1996, pp. 987–990.
[17] M. Y. Koledintseva, K. N. Rozanov, G. Di Fazio, and J. L. Drewniak, "Restoration of the Lorentzian and Debye curves of dielectrics and magnetics for FDTD modeling," in *Proc. 5th Int. Symp. Electromagnetic Compatibility*, Sorrento, Italy, Sep. 2002, pp. 687–692.
[18] M. Y. Koledintseva. Algorithm for the Lorentzian susceptibility function extraction. [Online]. Available: http://www.emclab.umr.edu/pdf/Formulas_Koledintseva.pdf
[19] M. Y. Koledintseva, G. Antonini, J. Zhang, A. Orlandi, K. N. Rozanov, and J. L. Drewniak, "Reconstruction of the parameters of Debye and Lorentzian dispersive media using a genetic algorithm," in *Proc. IEEE Int. Symp. Electromagnetic Compatibility*, vol. 2, Boston, MA, Aug. 2003, pp. 898–903.
[20] M. Y. Koledintseva, J. Wu, J. Zhang, J. L. Drewniak, and K. N. Rozanov, "Representation of permittivity for multiphase dielectric mixtures in FDTD modeling," in *Proc. IEEE Int. Symp. Electromagnetic Compatibility*, vol. 1, Santa Clara, CA, Aug. 2004, pp. 309–314.

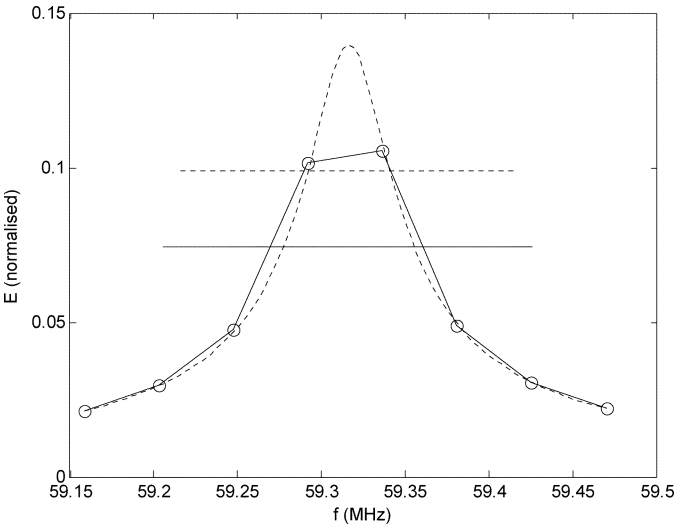

Fig. 1. Simulated frequency response of electric field strength in a screened room, showing how a linear interpolation leads to an overestimate of half-power bandwidth. (Solid line) Interpolated response. (Dotted line) "True" response.

Improved Determination of Q-Factor and Resonant Frequency by a Quadratic Curve-Fitting Method

M. P. Robinson and J. Clegg

***Abstract*—The Q-factor and peak frequency of resonant phenomena give useful information about the propagation and storage of energy in an electronic system and therefore its electromagnetic compatibility performance. However, the calculation of Q by linear interpolation of a discrete frequency response to obtain the half-power bandwidth can give inaccurate results, particularly if the data are noisy or the frequency resolution is low. We describe a more accurate method that makes use of the Lorentzian shape of the resonant peaks and involves fitting a second-order polynomial to the reciprocal power plotted against angular frequency. We demonstrate that this new method requires less than one quarter the number of frequency points as the linear method to give comparable accuracy in Q. The new method also gives comparable accuracy for signal-to-noise ratios that are approximately 8 dB greater. It is also more accurate for determination of peak frequency. Examples are given both from measured frequency responses and from simulated data obtained by the transmission line matrix method.**

***Index Terms*—Electromagnetic compatibility (EMC) measurements, interpolation, Q-factor, resonance, resonant frequency.**

I. Introduction

Resonant phenomena are encountered in the field of electromagnetic compatibility (EMC) when the dimensions of circuit boards, cables, screened enclosures, and other structures are large compared to the frequencies of interest. Although the Q-factors of these resonances are often neglected, they are actually of great significance because they describe the energy absorption and hence the height of the peaks in the frequency response. These are often more important than the exact frequencies of the resonances. Q is important in the energy-balance approach that Hill *et al.* take to characterizing the shielding effectiveness of large enclosures [1], while Dawson *et al.* have extracted peak parameters from frequency responses in order to validate computational electromagnetic (CEM) models [2]. The Q-factors of the individual modes are key parameters in the design of stirred-mode chambers and other reverberant environments [3]. Measurements of the changes in Q-factors and resonant frequencies are used to characterize the contents of shielded enclosures by means of the resonant perturbation technique [4]. In many cases, the data are obtained by either simulation or computer-controlled instrumentation, and consist of scalar values of voltage, electric field, etc. at discrete frequency points.

A simple and well-known method of calculating the Q from a peak in a frequency response is to find the maximum power, divide it by two, find the bandwidth at half-power, and divide this into the resonant frequency. This "traditional" method was well suited to analogue instrumentation that gives a continuous curve on a display as an output, and to graphical calculation techniques. However, with discrete frequency points and numerical calculations it can lead to errors in the resonant frequency, and more so in Q-factor, particularly if the sampled frequency points are sparse. This is because it is unlikely that a frequency point will lie exactly on the peak, so the peak power is underestimated, the bandwidth overestimated, and the Q is too low. Further errors come from linear interpolation between points—the method used in many automated network analyzers (ANAs). This is illustrated in Fig. 1, which shows how the bandwidth is overestimated owing to the poor frequency resolution. In this example, it is about 85% too high, and the peak frequency is also in error by 21 kHz.

A better approach is to use more of the points near the peak to improve accuracy. A technique that applies this idea to transmission (S_{21}) measurements of the Q of a cavity is described admirably by Leong and Mazierska [5]. Their method involves fitting a circle to complex S_{21} values plotted on a Smith Chart, and removes the effects of cables, connectors, and mismatches to give an accurate determination of Q-factors in the range 10^3–10^7. It is well-suited to precision metrology, in a setup where phase information is available. In the field of EMC, however, we often have to use scalar instruments or deal with data which could have been recorded alongside phase information but was not. There are often practical limits to the smallness of the frequency step. In computational electromagnetics, results from time-domain simulations are converted to the frequency domain by Fourier transforms giving discrete points. To improve the resolution means running the model for longer, which

Manuscript received May 13, 2004; revised September 1, 2004.
The authors are with the Physical Layer Group, Department of Electronics, University of York, York YO10 5DD, U.K.
Digital Object Identifier 10.1109/TEMC.2005.847411